

Protective effect of bone marrow-derived mesenchymal stem cells on methotrexate-induced brain and liver injury in female albino rats: Histological study

Hadwa Ali Abdel khalek, Heba Fikry, Sara Abdel Gawad

Histology & Cell Biology Department, Faculty of Medicine, Ain-Shams University, Cairo, Egypt
sara_elsebaey@med.asu.edu.eg

Abstract: Background and Objectives: Methotrexate (MTX) is an anti-folate drug that is widely used in the treatment of rheumatic disorders and malignant tumors. The efficacy of MTX is often limited by its severe side effects and toxic sequelae. Bone marrow derived mesenchymal stem cells (BM-MSCs) are a novel source for cell-based therapy and regenerative medicine. **Aim of the work:** to investigate the possible therapeutic effect of BM-MSCs therapy on MTX induced damage in brain and liver of female albino rats. **Materials and Methods:** Ten Wister male albino rats of average 100 gm were served as donors for stem cells obtained from their bone marrow for isolation of BM-MSCs. Forty Wister female adult albino rats of 200-250 gm were randomly and equally divided into four groups (10 animals each). **Group I (Control group):** Female rats were injected with phosphate buffer saline (PBS) and used to collect control brain & liver samples. **Group II (MTX group):** Female rats were injected intraperitoneally with MTX (0.5 mg /kg twice a week) for four weeks. **Group III (MSCs group):** Female rats were injected intraperitoneally with MTX as in group II for four weeks then received single intraperitoneal injection of 2×10^6 BM-MSCs suspended in PBS per rat and scarified after another four weeks. **Group IV (Recovery group):** Female rats were injected intraperitoneally with MTX as in group II for four weeks then allowed to survive for another successive four weeks without treatment then sacrificed. **Results:** Histological examination of the brain sections of MTX treated groups (groups II & IV) revealed shrunken deeply stained pyramidal cells of the frontal cortex with significant increase in the number of GFAP positive immuno-reactive astrocytes and caspase-3 immuno-reactive pyramidal cells in the frontal cortex as compared to that of the control group. Liver sections of MTX treated groups (groups II & IV) showed distorted hepatic architecture as most of the hepatocytes revealed vacuolated cytoplasm. Mallory trichrome stained sections of these groups showed significant increase of collagen fibers deposition comparable to that of the control group. Nevertheless, transplantation of BM-MSCs in group III led to marked improvement of the frontal cortex. Moreover, few GFAP positive immuno-reactive astrocytes and caspase-3 positive immuno-reactive pyramidal cells were detected in the frontal cortex of rats in the same group. Remarkable improvement was recorded in the liver sections of the same group as the normal hepatic architecture was restored. In addition few collagen fibers were observed in Mallory trichrome stained sections. **Conclusion:** BM-MSCs administration in MTX treated rats has enormous outcome in both brain and liver.

[Hadwa Ali Abdel khalek, Heba Fikry, Sara Abdel Gawad. **Protective effect of bone marrow-derived mesenchymal stem cells on methotrexate-induced brain and liver injury in female albino rats: Histological study.** *Stem Cell* 2017;8(1):100-111]. ISSN: 1945-4570 (print); ISSN: 1945-4732 (online). <http://www.sciencepub.net/stem>. 17. doi:[10.7537/marscj080117.17](https://doi.org/10.7537/marscj080117.17).

Keywords: Frontal cortex, Liver, Methotrexate, Bone marrow mesenchymal stem cells, Histology, Rats.

1. Introduction:

Methotrexate (MTX) is a folate antagonist which competitively inhibits dihydrofolate reductase enzyme so it interferes with the nucleic acid synthesis. Methotrexate is used in the treatment of different types of cancer, autoimmune disorders, psoriasis, and medical termination of pregnancy [1]. It is also used in the treatment of sarcoidosis, vasculitis, inflammatory bowel diseases, and severe refractory asthma [2].

It was found that MTX declines the antioxidant defense of the cell leading cells to become sensitized toward reactive oxygen species (ROS). Reactive oxygen species play an extensive role in promoting cell toward apoptosis. Moreover, MTX which is used in chemotherapy regimen does not distinguish normal cells from malignant cells and hence promotes even

normal cells toward apoptosis [3]. Methotrexate drug-induced oxidative stress is implicated as a mechanism of toxicity in different tissues and organ systems; including nervous systems, liver, kidney, and cardiovascular [4].

Neuroimaging studies of patients on chemotherapy treatment showed disturbances in both grey and white matter volumes with alterations in certain memory-associated areas of the brain [5]. A considerable number of cancer survivors who were treated with chemotherapy revealed impairments in cognition with respect to verbal and visually related memory tasks after chemotherapy course completion [6]. Although cancer patients usually complain of cognitive impairments prior to chemotherapy treatment [7], there is a significant clue to suggest that

chemotherapy treatment may induce cognitive deficits. Specifically, such cognitive impairments can also detect in cancer-free rats that were treated with drugs such as MTX, cyclophosphamide, and 5-fluorouracil [8,9].

With the widespread use of MTX, hepatotoxicity is considered one of the most important and crucial side effects. It has been reported that liver toxicity may occur as well in particular high doses or even following chronic administration of MTX [10].

Mesenchymal stem cells are a novel source for cell-based therapy and regenerative medicine. MSCs transplantation has been widely tested in different clinical trials of cardiovascular, immunological, and neurological diseases with satisfying outcomes. The regenerative potential of MSCs is attributed to their basic characteristics as stem cells and their therapeutic potential as drugs. Moreover, MSCs have the ability of self-renewal and differentiation into multiple cells types. They also have migration potential which is important in regenerative medicine due to numerous injection routes according to the damaged tissue or organ [11,12].

Therefore, the present study was conducted to investigate the possible damage produced by MTX on the brain and liver of female albino rats and to evaluate the ameliorative effects of BM-MSCs in alleviating this MTX induced damage.

2. Materials and methods:

Animals:

The experiments were performed on ten male Wistar albino rats of average 100 gm and forty female Wistar adult albino rats weighting 200–250 gm. The protocol was approved by the Institutional Animal Ethics Committee for Faculty of Medicine, Ain Shams University, Cairo, Egypt. The rats were maintained under standard laboratory conditions with natural light-dark cycle. They were allowed standard pellet diet and tap water ad libitum.

Experimental grouping:

Ten Wistar male albino rats were served as donors for stem cells obtained from their bone marrow for isolation of BM-MSCs. Forty Wistar female adult albino rats were randomly and equally divided into four groups (10 animals each).

Group I (Control group): Female rats were injected intraperitoneally with 0.5 ml PBS and used to collect control brain and liver samples.

Group II (MTX group): Female rats were injected intraperitoneally with MTX (0.5 mg /kg twice a week) for four weeks according to *Yozai et al.* [13].

Group III (MSCs group): Female rats were injected intraperitoneally with MTX as in group II for four weeks and then received single intraperitoneal injection of BM-MSCs (2×10^6 cells suspended in 0.5

ml PBS) according to *Maron et al.* [14] and scarified after another four weeks.

Group IV (Recovery group): Female rats were injected intraperitoneally with MTX as in group II for four weeks then allowed to survive for another successive four weeks without any treatment then sacrificed.

At the end of the experimental period, animals were sacrificed using ether anesthesia. Brain and liver specimens were collected and processed for histological study.

Culture and characterization of BM-MSCs:

Bone marrow was harvested by flushing the tibiae and femurs of 6 weeks old male Wistar albino rats with Dulbecco's modified Eagle's medium (DMEM) supplemented with 10% fetal bovine serum (purchased from Lonza Company, Switzerland). Bone marrow cells were resuspended in complete culture medium supplemented with 1% penicillin–streptomycin (purchased from Lonza Company, Switzerland). Cells were incubated at 37°C in 5% humidified CO₂ and were examined daily with an inverted microscope (Axiovert 100; Carl-Zeiss, Jena, Germany) to follow-up the growth of the cells and to detect any infection. Upon formation of large colonies (80–90% confluence); usually after 10–12 days; cultures were washed twice with PBS and the cells were trypsinized with 0.25% trypsin in 1mM EDTA for 5 min at 37°C. The cell suspension was centrifuged and the cell pellet was mixed with 0.1 ml of trypan blue. Cell suspension was dispensed on top of a hemocytometer slide. The number of viable and non-viable cells was counted then viable cells were subcultured at 4×10^3 cells/cm² and used for experiments after the third passage. Mesenchymal stem cells in culture were characterized by their adhesiveness and fusiform shape. Streptavidin-biotin immunoperoxidase technique was used to detect CD29 and CD44 (purchased from Labvision, New York, USA) as a marker of MSCs [15].

Histological and immunohistochemical examination:

Immediately after decapitation, female rats were dissected then brain and liver; from different groups; were quickly removed and fixed in 10% neutral buffered formalin. After fixation, specimens were dehydrated, cleared, and embedded in paraffin. Serial sections of 5 µm thicknesses were cut and mounted on clean slides. Brain sections were stained by haematoxylin and eosin (H & E) and immunohistochemical staining for both GFAP (to detect astrocytes) and caspase3 (to detect apoptosis). Both antibodies were purchased from Labvision, New York, USA. Liver sections were stained by H & E and Mallory trichrome stain [16].

PCR detection of male-derived BM-MSCs:

Genomic DNA was prepared from liver tissue homogenate of the rats in each group using QIAamp® DNA Mini and Blood Mini KIT, Germany. The presence or absence of the sex determination region on the Y chromosome male (sry) gene in recipient female rats was assessed by PCR. Primer sequences for sry gene (forward 5'-CATCGAAGGGTTAAAGTGCCA-3', reverse 5'-ATAGTGTGTAG-GTTGTTGTCC-3') were obtained from published sequences and amplified a product of 104 bp was purchased from (Sigma-USA). The PCR conditions were as follows: incubation at 94°C for 4 min; 35 cycles of incubation at 94°C for 50 s, 60°C for 30 s, and 72°C for 1 min; with a final incubation at 72°C for 10 min. Separation of PCR products was done using 2% agarose gel electrophoresis and stained with ethidium bromide. Positive (male Wistar albino rat genomic DNA) and negative (female Wistar albino rat genomic DNA) controls were included in each assay. Y chromosomes marker was detected as transilluminated line [17].

Morphometric measurements:

In the brain sections, the following parameters were measured:

1. The area percentage of immuno-reactive star-shaped astrocytes stained by GFAP in the frontal cortex.

2. The number of pyramidal cells with positive brownish caspase-3 immuno-reaction in the frontal cortex.

In the liver sections, the area percentage of collagen content using Mallory trichrome stained sections was measured.

All the measurements were taken at high-power fields (HPFs) of magnification ($\times 400$).

From each group five different high power fields/section for both brain and liver were chosen to measure the mentioned parameters. An image analyzer Leica Q win V.3 program installed on a computer in the Histology & Cell Biology Department, Faculty of Medicine, Ain Shams University was used. The computer was connected to a Leica DM2500 microscope with built-in camera (Leica Microsystems GmbH, Ernst-Leitz-StraBe, Wetzlar, Germany).

Statistical Analysis:

All the collected data were revised and subjected to statistical analysis using one-way analysis of variance performed with SPSS.21 program (IBM Inc., Chicago, Illinois, USA) analysis for variance (ANOVA)-one way analysis and post-Hoc least significant difference (LSD). The differences were considered significant when p value was less than 0.05, and p value greater than 0.05 was considered non significant. Summary of the data was expressed as mean + standard deviation (SD).

3. Results:

Table 1. Mean \pm SD of area % of positive GFAP immune-reaction, number of caspase-3 +ve immuno-reactive cells/HPFs, and area % of collagen fibers in different groups.

	Group I	Group II	Group III	Group IV
Mean \pm SD of area% of positive GFAP immune reaction	0.89 \pm 0.08	4.5 \pm 0.71 (*▲)	1.1 \pm 0.14 (■○)	4.7 \pm 1.25 (*▲)
Mean \pm SD of number of caspase-3+ve immunoreactive cells	7.1 \pm 1.16	46.8 \pm 3.86 (*▲)	9.8 \pm 1.83 (■○)	47.1 \pm 2.78 (*▲)
Mean \pm SD of area% of collagen fibers	13.2 \pm 2.5	73.2 \pm 3.36 (*▲)	20.4 \pm 3.3 (■○)	74.4 \pm 2.7 (*▲)

*Significant difference from group I. ■ Significant difference from group II.

▲ Significant difference from group III. ○ Significant difference from group IV.

Primary culture of bone marrow-derived mesenchymal stem cells results:

On day 10, examination of primary culture of BM-MSCs using an inverted light microscope showed the attached cells appeared forming colonies with granular cytoplasm and interdigitating cytoplasmic processes (Fig. 1A). Characterization of the cultured cells on day 10 using CD29 and CD44 revealed positive brownish reaction in some of the attached cells (Fig. 1B,1C) respectively.

Histological and morphometric results of the brain:

Haematoxylin and eosin stained sections of the frontal cortex of rats of group I (control group)

showed the layers of the cerebral cortex; the outer molecular layer, the external granular layer, external pyramidal layer, the inner granular layer, the inner pyramidal, and the polymorphic layer (Fig. 1D). The pyramidal cells of the external pyramidal layer presented open face nuclei and basophilic cytoplasm. The smaller neuroglia with small dark nuclei cells were scattered in between the neuronal cells (Fig. 2A). Frontal cortex sections of rats of group II (MTX group) revealed shrunken pyramidal cells with deeply acidophilic cytoplasm and intensely stained nuclei (Fig. 2B). In the frontal cortex sections of the rats in co-treated MTX with BM-MSCs group (group III),

marked improvement was recorded as nearly all of the pyramidal cells exhibited open face nuclei (**Fig. 2C**). Brain sections of rats in **group IV** (recovery group) showed marked neuronal damage in the frontal cortex

as the pyramidal cells appear shrunken with deeply acidophilic cytoplasm and intensely stained nuclei with peri-neuronal halos. The interstitium appeared highly vacuolated (**Fig. 2D**).

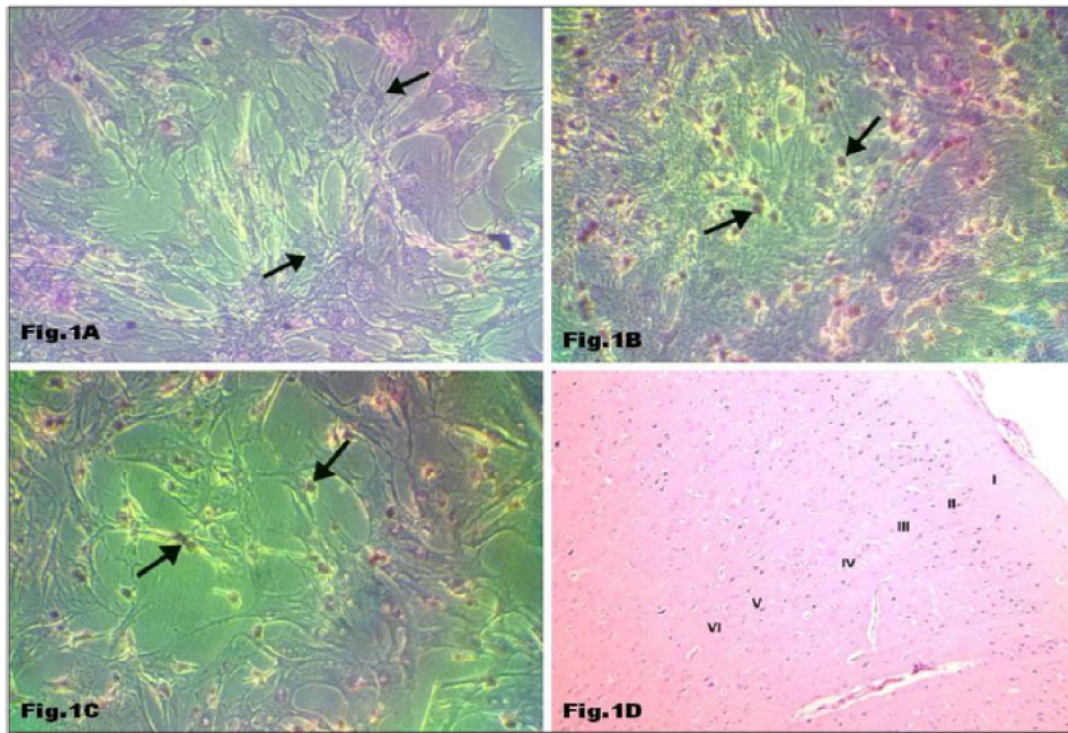


Figure 1: (A) Primary culture of BM-MSCs on day ten showing attached cells forming colonies with granular cytoplasm and interdigitating processes (↑) (**Inverted microscope X 200**). (B) Tertiary culture of BM-MSCs on day ten showing some of the attached cells reveal positive brownish immune-reaction for CD-29 (↑) (**Inverted microscope, Streptavidin-biotin peroxidase X200**). (C) Tertiary culture of BM-MSCs on day ten showing some of the attached cells exhibit positive brownish immune-reaction for CD-44 (↑) (**Inverted microscope, Streptavidin-biotin peroxidase X200**). (D) Section of the frontal cortex showing the upper five layers of the frontal cortex: the outer molecular layer I, external granular layer II, external pyramidal layer III, inner granular layer IV, inner pyramidal layer V, and polymorphic layer VI (**Group I H & E X100**).

Immunohistochemical analysis using GFAP antibodies in the control **group I** demonstrated few cytoplasmic immuno-reactive astrocytes dispersed in between the pyramidal cells of the frontal cortex (**Fig. 3A**). However, brain sections of rats of **group II** showed significant increase ($P < 0.05$) in the number of GFAP immuno-reactive astrocytes in the frontal cortex as compared to that of the control **group I** (**Fig. 3B**) (**Table 1**). Sections of the frontal cortex of rats in **group III** (BM-MSCs group) displayed few GFAP immuno-reactive astrocytes (**Fig. 3C**) as there was significant decrease ($P < 0.05$) in their number comparable to that of **group II** (**Table 1**). Whereas, **Group IV** (recovery group) exhibited significant increase ($P < 0.05$) in the number of astrocytes with positive cytoplasmic immune-reaction in the frontal cortex as compared to that of **group III** (**Fig. 3D**) (**Table 1**).

Immunohistochemical analysis of caspase-3 in the control **group I** displayed few cells with positive nuclear immune-reaction in the frontal cortex (**Fig. 4A**). MTX treated rats in **group II** showed significant increase ($P < 0.05$) in the number of caspase-3 immune-reactive pyramidal cells of the frontal cortex as compared to that of **group I** (**Fig. 4B**) (**Table 1**). Meanwhile, BM-MSCs administration in **group III** revealed significant decrease ($P < 0.05$) in the number of caspase-3 immune-reactive pyramidal cells comparable to that of **group II** (**Fig. 4C**) (**Table 1**). The frontal cortex of rats in **group IV** (recovery group) displayed significant increase ($P < 0.05$) in the number of caspase-3 positively stained pyramidal cells as compared to that of **group III** (**Fig. 4D**) (**Table 1**).

Histological and morphometric results of the liver:

Examination of H & E stained sections of the control liver (**group I**) revealed intact classical hepatic

lobules; hepatocytes were arranged in the form of branching and anastomosing plates radiating from the central veins and were separated by blood sinusoids which were lined by flat endothelial cells. The hepatocytes displayed acidophilic cytoplasm with single central rounded vesicular nuclei whereas, some of the hepatocytes appeared binucleated (**Fig. 5A**). In MTX treated rats (**group II**); histopathological changes were detected in the form of distorted hepatic architecture as most of the hepatocytes revealed vacuolated cytoplasm together with areas of mononuclear cellular infiltration (**Fig. 5B**). Administration of BM-MSCs in **group III** revealed remarkable improvement as the normal hepatic architecture was restored and the hepatocytes appeared nearly similar to that of the control rats (**Fig. 5C**). Nevertheless, sections of the recovery group (**group IV**) still displayed marked affection of the liver tissue as there was loss of the usual hepatic architecture. The hepatocytes presented with highly vacuolated cytoplasm and deeply stained nuclei. Blood sinusoids appeared dilated (**Fig. 5D**).

In Mallory trichrome stained sections, the liver parenchyma of the control group (**group I**) appeared

to be supported with a stroma of very delicate meshwork of collagen fibers. Few collagen fibers appeared surrounding the central veins, in portal area, and in capsule (**Fig. 6A**). However, MTX treatment in **group II** resulted in significant increase ($P<0.05$) in the area percentage of collagen fibers as compared to that of the control **group I** (**Fig. 6B**) (**Table 1**). In liver sections of co-treated MTX with BM-MSCs group (**group III**), there was significant decrease ($P<0.05$) in the area percentage of collagen fibers comparable to that of **group II** (**Fig. 6C**) (**Table 1**). Whereas, liver sections of **group IV** exhibited significant increase ($P<0.05$) in the area percentage of collagen fibers as compared to that of **group III** (**Fig. 6D**) (**Table1**).

PCR detection of male-derived BM-MSCs in liver sections:

The SRY gene which was used as Y chromosome marker was detected in male rats from which BM-MSCs were isolated. It was also expressed in female rats which were received male derived BM-MSCs in MSCs group (group III). However, Y chromosome marker was not detected in the control group, MTX group, and recovery group (**Fig. 7**).

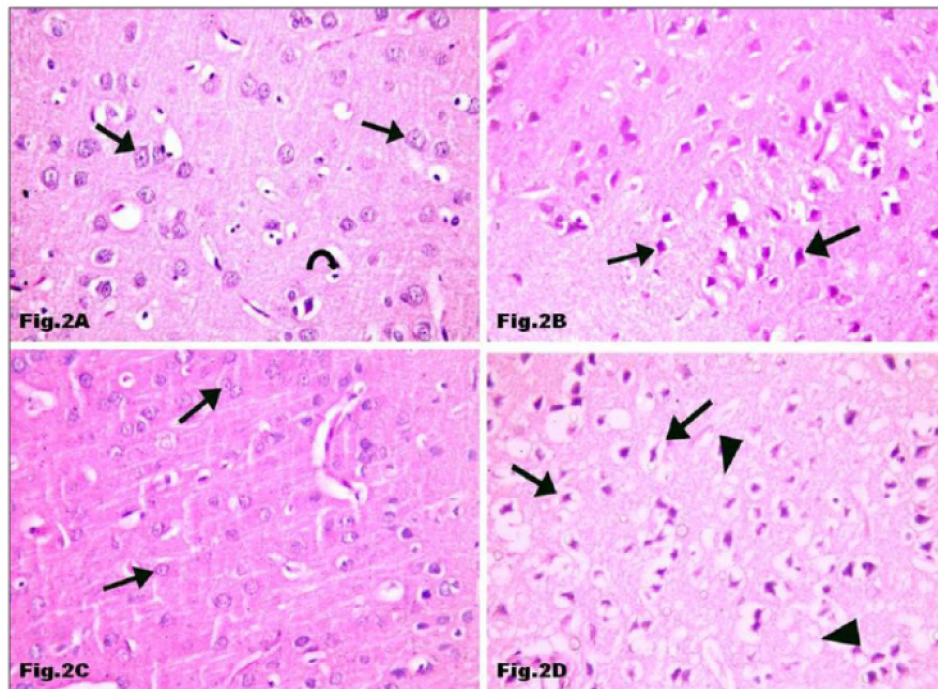


Figure 2: (A) Section of the frontal cortex showing the pyramidal neurons with their open face nuclei (↑). Neuroglia appears in between the pyramidal neurons with their smaller dark nuclei (curved arrow) (Group I). (B) Section of the frontal cortex showing most of the pyramidal cells appears shrunken with intensely acidophilic cytoplasm and deeply stained nuclei (↑) (Group II). (C) Section of the frontal cortex showing nearly all of the pyramidal cells appear with open face nuclei (↑) (Group III). (D) Section of frontal cortex showing most of the pyramidal neurons appears shrunken and revealed deeply acidophilic cytoplasm and darkly stained nuclei with peri-neuronal halos (↑). Notice the vacuolated interstitium (▲) (Group IV). (H & E X 640)

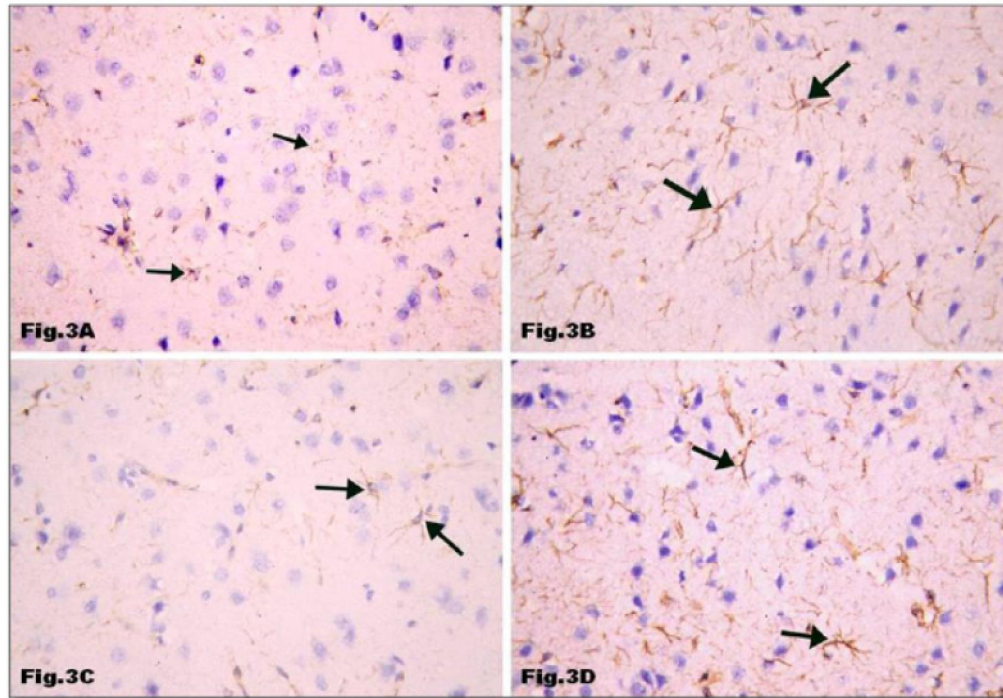


Figure 3: (A) Section of the frontal cortex showing few scattered GFAP positive astrocytes (↑) (Group I). (B) Section of the frontal cortex showing numerous GFAP immune-reactive astrocytes (↑) with long cytoplasmic processes (Group II). (C) Section of the frontal cortex showing only few dispersed astrocytes appear with GFAP immune-reaction (↑) (Group III). (D) Section of the frontal cortex showing many astrocytes with positive immune-reaction for GFAP (↑) (Group IV). (Avidin biotin peroxidase for GFAP X 640)

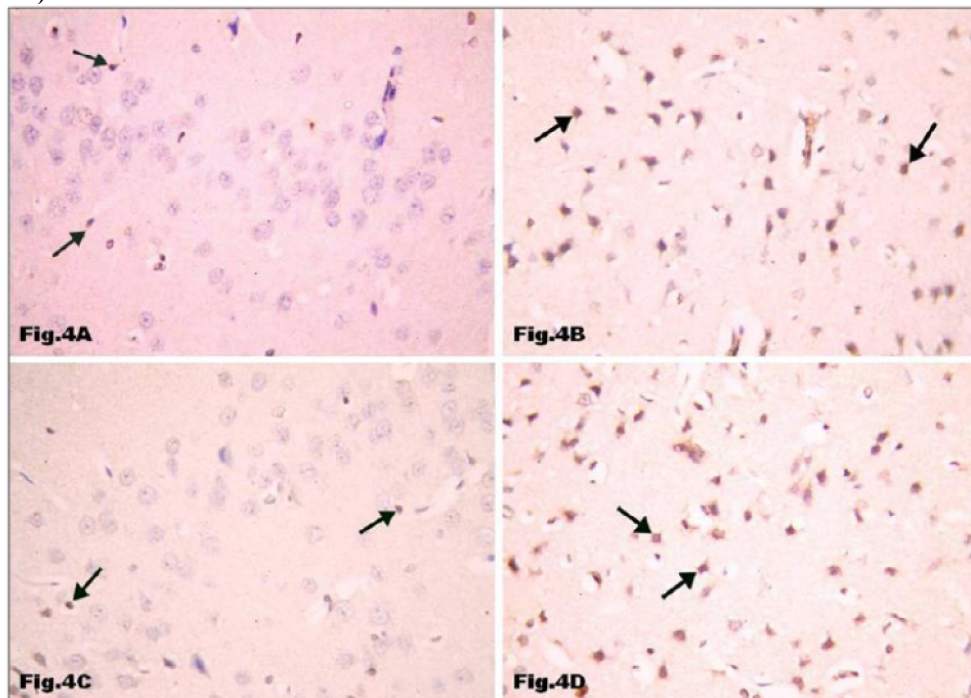


Figure 4: (A) Section of the frontal cortex showing caspase-3 immune-reaction in the nuclei of few pyramidal cells (↑) (Group I). (B) Section of the frontal cortex showing positive brownish caspase-3 immune-reaction in many pyramidal cells (↑) (Group II). (C) Section of the frontal cortex showing only few scattered pyramidal cells appear with positive caspase-3 immune-reaction (↑) (Group III) (D) Section of the frontal cortex showing most of the pyramidal cells exhibit positive caspase-3 immune-reaction (↑) (Group IV). (Avidin biotin peroxidase for caspase-3 X 640)

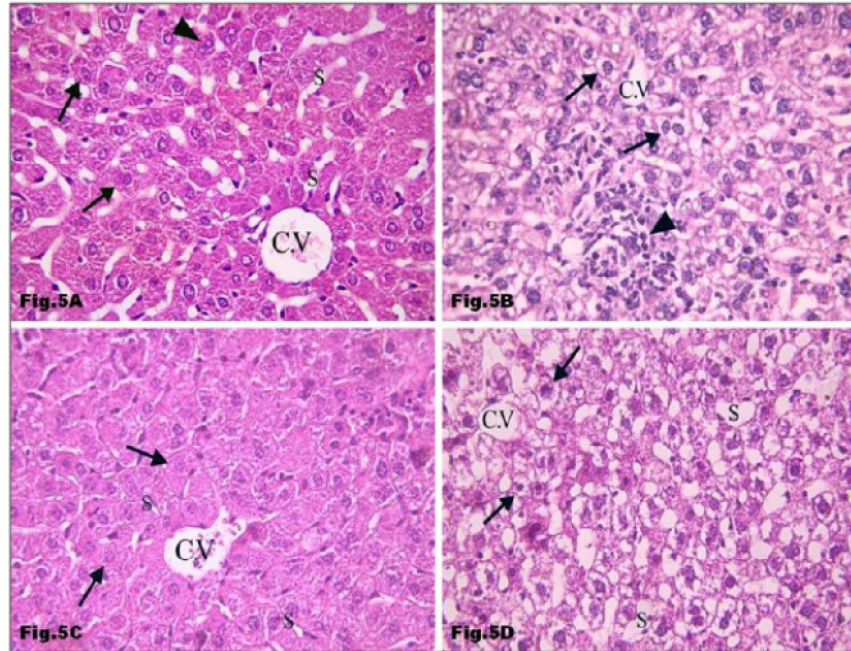


Figure 5: (A) Section of the liver showing plates of hepatocytes radiating from the central vein (C.V) and separated by blood sinusoids (S). The hepatocytes have central, rounded, vesicular nuclei with acidophilic cytoplasm (↑) and some of them appear binucleated (▲) (Group I). (B) Section of the liver showing distorted hepatic architecture as most of the hepatocytes reveal vacuolated cytoplasm (↑). Mononuclear cellular infiltration (▲) could be obviously seen. Notice the central vein (C.V) (Group II). (C) Section of the liver showing restoration of the normal hepatic architecture as the plates of hepatocytes appear radiating from the central vein (C.V). The hepatocytes appear with vesicular nuclei and acidophilic cytoplasm (↑) and separated by blood sinusoids (S) (Group III). (D) Section of the liver showing distorted hepatic architecture as the hepatocytes exhibit highly vacuolated cytoplasm and darkly stained nuclei (↑). Blood sinusoids appeared dilated (S). Notice the central vein (C.V) (Group IV). (H & E X 640)

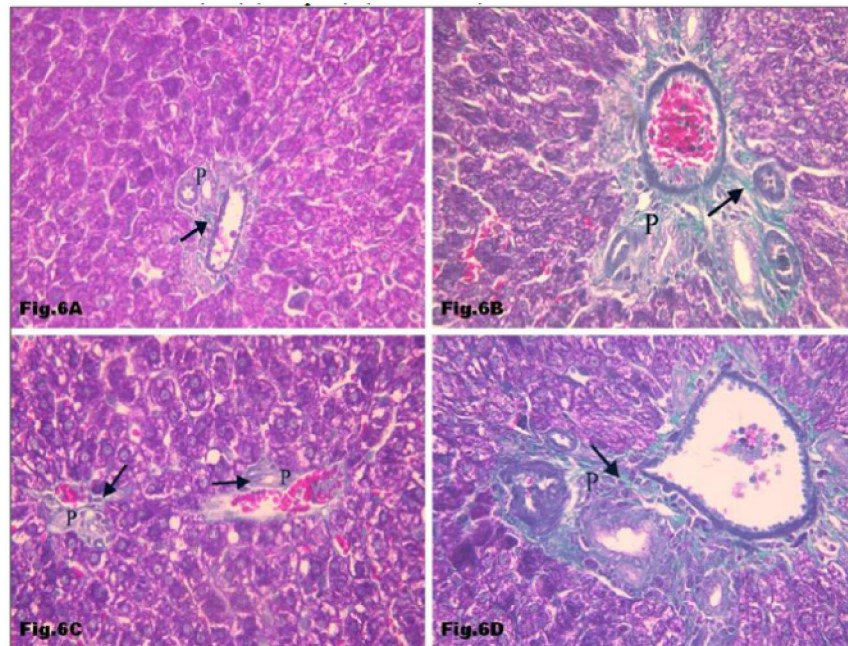


Figure 6: (A) Section of the liver showing few collagen fibers (↑) appear surrounding the portal area (P) (Group I). (B) Section of the liver showing extensive deposition of collagen fibers (↑) appear around the portal area (P) (Group II). (C) Section of the liver showing few collagen fibers (↑) could be seen round the portal area (P) (Group III). (D) Section of the liver showing massive collagen fiber (↑) deposition around the portal area (P) (Group IV). (Mallory trichrome X640)

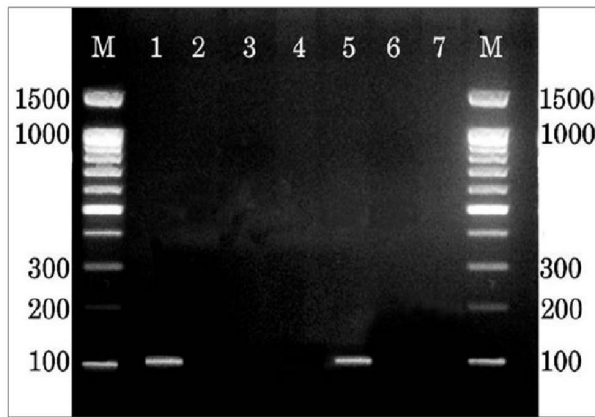


Figure 7: Showing presence of Y chromosome in male rats from which BM-MSCs were isolated (lane 1) and female rats treated with BM-MSCs in group III (lane 5). Y chromosome marker is not expressed in female rats of the control group I (lane 3), group II (lane 4) and group IV (lane 6). M: PCR marker (U.V. trans-illumination).

4. Discussion:

Methotrexate is a drug of choice and most widely used for the treatment of various types of cancers and autoimmune diseases [1]. Its clinical use is limited due to its several side effects as neurotoxicity, hepatotoxicity, nephrotoxicity, and gastrointestinal toxicity [18, 19, 20, 21].

The current study revealed several histological changes in the frontal cortex and liver in both groups which were treated with MTX; group II and group IV. The mechanism of MTX toxicity can be explained by its ability to competitively inhibit dihydrofolate reductase enzyme hence it interferes with the nucleic acid synthesis and cell proliferation, which results in cell apoptosis [22]. Methotrexate-induced apoptosis is considered to be mediated by the up-regulation of p53 and p21 proteins and expression of the CD95 receptor/ligand system [23]. The oxidative stress is another well-known mechanism that plays a vital role in MTX toxicity [10] which consequently results in shape and structural changes of the nucleus by causing DNA fragmentation and denaturation hence the initiation of apoptosis [22].

It has previously been assumed that systemic chemotherapy could not cross the blood brain barrier and so would have few side effects on the brain. Currently, it has been delineated that many chemotherapy agents; including MTX; can access the brain in significant concentrations, when administered in high doses [24]. Additionally, systemic chemotherapy can elicit extensive cognitive malfunction; often referred to as "chemobrain"; a

condition that can persist for a long time after treatment [25].

The present study was conducted on the frontal cortex which is critically implicated in several aspects of learning and memory. The frontal cortex is also involved in working memory and concerned in the temporal ordering of spatial and non-spatial events as well as to the organization and planning of responses [26]. In MTX treated groups; group II and group IV, considerable histological changes were detected in the frontal cortex as the pyramidal cells appeared shrunken with deeply acidophilic cytoplasm and intensely stained pyknotic nuclei. These findings suggested MTX induced neuro-degenerative changes and was confirmed by a significant increase in the number of caspase-3 immune-reactive cells as compared to that of the control group. In agreement, anticancer drugs were recorded to adversely affect the self-renewal potential of the neural progenitor cells and also chromatin remodeling [27]. Additionally, Yang *et al.* [28] detected that MTX treated mice exhibited a significant depression-like behaviors and memory defects together with an increase in active caspase-3 expression in the hippocampus. Bhojwani *et al.* [29] added that, the mechanism of chemotherapy induced neurotoxicity is likely attributable to either disruption of CNS folate homeostasis and/or direct neuronal damage.

Astrocytes are cellular residents of CNS involved in preserving the neuronal function and homeostasis and, like microglia, respond to many CNS insults [30]. In the current study, the frontal cortex of MTX treated rats displayed a significant increase in the area percentage of astrocytes immuno-reaction expression and these findings were similar to [31,32,30].

Concerning MTX induced hepatotoxicity; several histological changes were detected in both groups II & IV (MTX-treated groups) as there was distorted hepatic architecture, vacuolated hepatocytes, and inflammatory cells infiltration. Similar results were also reported by [33, 10, 34]. Barker *et al.* [35] added that, prolonged use of MTX leads to retention of polyglutamate forms of the drug in the hepatocytes with subsequent intracellular storage of MTX resulting in slowing of the drug clearance and providing a depot that extends the duration of the drug exposure.

Regarding the area percentage of collagen fibers in MTX treated groups (group II and group IV); the current study reported a statistically significant increase in this parameter comparable to that of the control group. Similar results were also observed by Tousson *et al.* [36]. Such hepatic fibrosis seemed to be attributable to direct toxic effect of MTX as it induces proliferation of the hepatic fibrous connective tissue stroma [37]. Also, Hytioglu *et al.* [38]

reported that MTX is well known to cause liver fibrosis in some patients, which might progress to cirrhosis.

Examination of the frontal cortex of co-treated MTX with BM-MSCs group (group III) showed nearly all of the pyramidal cells appear healthy with open face nuclei together with a significant decrease in the area percentage of astrocytes immune-reaction expression in comparison to that of MTX treated groups (groups II & IV). Additionally, a significant decrease in the number of caspase-3 immune-reactive cells was detected in this group comparable to that of both groups II & IV. Similarly, **Zickri1 et al. [39]** demonstrated that human cord blood MSCs therapy revealed ameliorating effects on Adriamycin induced chemobrain in an experimental rat model. Moreover, **Donega et al. [40]** also noticed decline in the amount of GFAP +ve expressing cells after 15 days of MSCs treatment in ischemic brain injury in mice, which suggests the ability of MSCs to diminish gliosis. Accordingly, intrathecal administration of MSCs by lumbar puncture might be useful for treatment of brain injuries, such as stroke, or neurodegenerative disorders **[41]**. Another study demonstrates that stem cells isolated from the adipose tissue and umbilical cord release trophic/neuroregulatory factors that improve the metabolic viability and neuronal cell densities in primary cultures of hippocampal neurons **[42]**. Furthermore, **Da Silva et al. [43]** delineated that MSCs have been shown to selectively migrate to and settle in injured tissue and this “homing” capacity can explain the ability of stem cells to reach delicate sites, such the brain or the heart. Many mechanisms have been put forth to explain MSCs' homing behaviour. For instance, MSCs' migration is influenced by several chemokines and growth factors **[44]**. Another mechanism is the adhesion of MSCs to the injured tissue endothelium due to vascular cell adhesion molecule (VCAM) expression in a manner similar to the homing mechanism of leukocytes **[45]**.

Moreover, the ability of neurotherapeutic drugs to cross the blood brain barrier (BBB) is crucial for their proper potency **[46]**. Recent researches have indicated that MSCs might already possess the ability to cross the BBB **[47]**. **Steingen et al. [48]** identified the mechanisms through which this occurs. They suggested that, after coming into the contact with endothelium, MSCs leave the blood stream and integrate into the endothelium via the adhesion molecules VCAM-1/VLA-4 and $\beta 1$ integrin. After crossing the endothelial barrier, MSCs invade the host tissue by the use of plasmic podia. Furthermore, **Matsushita et al. [49]** reported that, despite the presence of tight junctions in the BBB, MSCs; similar to lymphocytes; seem to influence tight junction

barrier properties leading to their transient abolishment.

In addition, evidence suggests that MSCs protect and repair the damaged CNS via multiple mechanisms. For example, MSCs implanted into mouse hippocampus were found to enhance the proliferation, migration, and differentiation of native neural stem cells (NSCs) through chemokines that released by MSCs themselves or indirectly through activating the surrounding astrocytes **[43]**. Another mechanism is the neural differentiation potential of MSCs into neuron-like and glial-like cells **[50]**. MSCs also show immunomodulatory capacities by interacting with a wide range of immune cells; probably through a cell-to-cell contact mechanism; therefore they are able to suppress the proliferative response of the lymphocytes **[51]**. **Donega et al. [40]** hypothesized that MSCs stimulate microglia polarization towards M₂ phenotype; which promote tissue repair and anti-inflammation.

Furthermore, MSCs act as an implanted biopharmacy as they synthesize and release a broad range of bioactive molecules **[52]** such as anti-inflammatory cytokines, trophic and growth factors, interleukin IL-6, IL-7, IL-8, IL-11, IL-15, macrophage colony-stimulating factor, and stem-cell factor **[53]**, which consecutively activate endogenous restorative mechanisms within the injured tissues.

Examination of liver sections of co-treated MTX with MSCs group showed restoration of the normal hepatic architecture together significant reduction in the area percentage of collagen fibers in the liver sections of this group comparing to this of both groups II & IV. Similarly, **Prockop et al. [54]** detected that MSCs can repair hepatic tissues through differentiation into the phenotype of the damaged cells and secretion of cytokines and growth factors which enhance the repair of hepatic cells and regulate the local immune system, apoptosis, fibrosis, and angiogenesis. Furthermore, it has been demonstrated that bone marrow MSCs conditioned medium has antiapoptotic and pro-mitotic effects on cultured hepatocytes **[55]**. **Berardis et al. [55]** added that, systemic infusion of MSCs conditioned medium could inhibit hepatocyte cell death and enhance liver regeneration *in vivo*, in a rat model of acute liver injury. Additionally, **Jin et al. [56]** reported that MSCs transplantation could regenerate the reduction in hepatic protective genes. It was also determined that in ischemic/perfusion damage to liver, MSCs transplantation could induce suppression of oxidative stress and apoptosis in rats. Moreover, MSCs have been shown to be effective in reducing the fibrotic area in lung and heart with good outcomes **[57, 58]**. This effect was attributable to their secretory profile as

they are known to secrete several anti-fibrotic molecules such as hepatocyte growth factor [55].

Conclusion and recommendations

Our previous results revealed deleterious effects of MTX on the structure of both the brain and liver. Nevertheless, it was assumed that BM-MSCs transplantation in MTX treated rats has enormous outcomes in the brain and liver.

Further researches are still required for better understanding the mode of action of BM-MSCs and their trophic effects on the injured tissue. Moreover, investigations are also needed concerning the timing of cells' administration and the threshold number of transplanted cells in order to be able to employ them efficiently in the clinical applications.

Conflicts of interest

There are no conflicts of interest.

References

1. Khan ZA, Tripathi R, Mishra B., 2012. Methotrexate: a detailed review on drug delivery and clinical aspects. *Expert Opin Drug Deliv.* 9:151–169.
2. Hadi N, Al-Amran F, Swadi A, 2012. Metformin ameliorates methotrexate-induced hepatotoxicity. *J Pharmacol Pharmacother.* 3(3): 248–253.
3. Ali N, Rashid S, Nafees S, Hasan S K, Sultana S., 2014. Beneficial effects of Chrysin against Methotrexate-induced hepatotoxicity via attenuation of oxidative stress and apoptosis. *Mol Cell Biochem.* 385:215–223.
4. Deavall D, Martin E, Horner J, Roberts R., 2012. Drug-induced oxidative stress and toxicity. *J. Toxicol.* 2012:1-13.
5. Lyons L, El Beltagy M, Umka J, Markwick R, Startin C, Bennett G, Wigmore P., 2011. Fluoxetine reverses the memory impairment and reduction in proliferation and survival of hippocampal cells caused by methotrexate chemotherapy *Psychopharmacology* 215:105–115.
6. Vardy J, Tannock I., 2007. Cognitive function after chemotherapy in adults with solid tumours. *Crit Rev Oncol Hematol.* 63:183–202.
7. Ahles TA, Saykin AJ, McDonald BC, Furstenberg CT, Cole BF, Hanscom B S, Mulrooney T J, Schwartz G N, Kaufman P A., 2008. Cognitive function in breast cancer patients prior to adjuvant treatment. *Breast Cancer Res Treat.* 110:143–152.
8. Foley J, Raffa R, Walker E, 2008. Effects of chemotherapeutic agents 5-fluorouracil and methotrexate alone and combined in a mouse model of learning and memory. *Psychopharmacology* 199: 527–538.
9. Seigers R & Fardell J, 2011. Neurobiological basis of chemotherapy-induced cognitive impairment: a review of rodent research. *Neurosci Biobehav Rev.* 35:729–741.
10. Kose E, Sapmaz H, Sarihan E, Vardi N, Turkoz Y, Ekinici N, 2012. Beneficial Effects of Montelukast Against Methotrexate-Induced Liver Toxicity: A Biochemical and Histological Study. *The Scientific World Journal.* Article ID 987508.
11. Chamberlain G, Fox J, Ashton B, Middleton J., 2007. Concise review: mesenchymal stem cells: their phenotype, differentiation capacity, immunological features, and potential for homing. *Stem Cells* 25:2739-2749.
12. Gebler A, Zabel O, Seliger B., 2012. The immunomodulatory capacity of mesenchymal stem cells. *Trends Mol Med.* 18:128-134.
13. Yozai K, Shikata K, Sasaki M, Tone A, Ohga S, Usui H., 2005. Methotrexate prevents renal injury in experimental diabetic rats via anti-inflammatory actions. *J Am Soc Nephrol.* 16: 3326- 3338.
14. Maron-Gutierrez T, Castiglione RC, Xisto DG, Oliveira MG, 2011. Bone marrow-derived mononuclear cell therapy attenuates silica-induced lung fibrosis. *Eur Respir J.* 37(5):1217–1225.
15. Abdel Aziz M, Atta H, Mahfouz S, Fouad H, Roshdy N, Ahmed H, Rashed L, Sabry D, Hassouna A., 2007. Therapeutic potential of bone marrow-derived mesenchymal stem cells on experimental liver fibrosis. *Clinical Biochemistry* 40: 893–899.
16. Bancroft JD, Layton C, Suvarna SK, 2013. *Bancroft's Theory and Practice of Histological Techniques.* 7th ed. Elsevier Churchill Livingstone: London, United Kingdom; pp. 386–535.
17. An J, Beauchemin N, Albanese J, Abney T O, Sullivan A K.1997. Use of a rat cDNA probe specific for the Y chromosome to detect male-derived cells. *J Androl.* 18:289–293.
18. Vardi N, Parlakpınar H, Ozturk F et al. 2008. Potent protective effect of apricot and beta-carotene on methotrexate-induced intestinal oxidative damage in rats. *Food Chem Toxicol.* 46:3015–3022.
19. Abraham P, Kolli VK, Rabi S., 2010. Melatonin attenuates methotrexate-induced oxidative stress and renal damage in rats. *Cell Biochem Funct.* 28:426–433.
20. Zhao X, Shu G, Chen L et al., 2012. A flavonoid component from *Docynia delavayi* (Franch.)

- Schneid represses transplanted H22 hepatoma growth and exhibits low toxic effect on tumor-bearing mice. *Food Chem Toxicol.* 50:3166–3173.
21. Ng LC, Lee YY, Lee CK et al. 2013. A retrospective review of methotrexate-induced hepatotoxicity among patients with psoriasis in a tertiary dermatology center in Malaysia. *Int J Dermatol.* 52:102–105.
 22. Vardi N, Parlakpınar H, Cetin A, Erdogan A, Ozturk C., 2010. Protective Effect of beta - Carotene on Methotrexate-Induced Oxidative Liver Damage. *Toxicologic Pathology* 38: 592-597.
 23. Sun J, Sugiyama A, Inoue S, Takeuchi T, Furukawa S., 2014. Effect of Methotrexate on Neuroepithelium in the Rat Fetal Brain. *J. Vet. Med. Sci.* 76(3): 347–354.
 24. Lassman A, Abrey L, Shah G, Panageas K, Begemann M, Malkin M, Raizer J., 2006. Systemic high-dose intravenous methotrexate for central nervous system metastases. *J Neuro-Oncol.* 78:255–260.
 25. Acharya M, Martirosian V, Chmielewski N, Hanna N, Tran K, Liao A, Christie L, Parihar V, Charles L., 2015. Stem Cell Transplantation Reverses Chemotherapy-Induced Cognitive Dysfunction. *Cancer Res.* 75(4):676-686.
 26. Adekomi A, Adewale O, Muhameed O, Aghaje A, Oyesomi T, 2013. Neuronal alterations in the prefrontal cortex of rats with carbon tetrachloride (CCl₄) induced hepatic damage. *Journal of Clinical Pathology and Forensic Medicine* 4 (1): 6-14.
 27. Briones TL, Woods J., 2011. Chemotherapy-induced cognitive impairment is associated with decreases in cell proliferation and histone modifications. *BMC Neurosci.* 12:124.
 28. Yang M, Kim J S, Kim J, Kim S H, Kim J C, Kim J, Wang H, Shin T, Moon C., 2011. Neurotoxicity of methotrexate to hippocampal cells in vivo and in vitro. *Biochem Pharmacol.* 82(1):72-80.
 29. Bhojwani D, Sabin N D, Pei D, Yang JJ, Khan R B, Panetta J C, Krull K R, Inaba H, Rubnitz J E, Metzger M L, Howard S C, Ribeiro R C, Cheng C, Reddick W R, Jeha S, Sandlund J T, Evans W E, Pui C H, Relling M V., 2014. Methotrexate-Induced Neurotoxicity and Leukoencephalopathy in Childhood Acute Lymphoblastic Leukemia. *J Clin Oncol.* 32(9): 949–959.
 30. Feiock C, Yagi M, Maidman A, Rendahl A, Hui S, Seeling D., 2016. Central nervous system injury- a newly observed bystander effect of radiation. *PLoS ONE* 11(9): e0163233. doi.10.1371.
 31. Semmler A, Okulla T, Sastre M, Dumitrescu-Ozimek L, Heneka MT., 2005. Systemic inflammation induces apoptosis with variable vulnerability of different brain regions. *J Chem Neuroanat.* 30: 144-157.
 32. Fardell J E, Zhang J, De Souza R, Vardy J, Johnston I, et al., 2014. The impact of sustained and intermittent docetaxel chemotherapy regimens on cognition and neural morphology in healthy mice. *Psychopharmacology (Berl)* 231: 841-852.
 33. Al-Motabagani M K., 2006. Histological and Histochemical Studies on the Effects of Methotrexate on the Liver of Adult Male Albino Rat. *Int. J. Morphol.* 24(3):417-422.
 34. Moghadam A R, Tutunchi S, Namvaran-Abbas-Abad A, Yazdi M, Bonyadi F, Mohajeri D, Mazani M, Marzban H, J. Los M and Ghavami S., 2015. Pre-administration of turmeric prevents methotrexate-induced liver toxicity and oxidative stress. *BMC Complementary and Alternative Medicine.* 15:246.
 35. Barker J, Horn E J, Lebowhl M, Warren R B, Nast A, Rosenberg W, Smith C., 2011. Assessment and management of methotrexate hepatotoxicity in psoriasis patients: report from a consensus conference to evaluate current practice and identify key questions toward optimizing methotrexate use in the clinic. *JEADV.* 25: 758–764.
 36. Tousson E, Zaki Z T, Abu-Shaer W A, Hassan H., 2014. Methotrexate-induced Hepatic and Renal Toxicity: Role of L-carnitine in Treatment. *Biomedicine and Biotechnology,* 2(4):85-92.
 37. Ros S, Juanol X, Condom E, Canas C, Riera J, Guardiola J, Del Blanco J, Rebasa P, Valverde J, Roig-Escofet O., 2002. Light and electron microscopic analysis of liver biopsy samples from rheumatoid arthritis patients receiving long-term methotrexate therapy. *Scand J Rheumatol.* 31 (6): 330-336.
 38. Hytiroglou P, Tobias H, Saxena R, Abramidou M, Papadimitriou CS, Theise N D., 2004. The canals of hering might represent a target of methotrexate hepatic toxicity. *Am J Clin Pathol.* 121 (3): 324-329.
 39. Zickri1 M B, Abd El Aziz D H, Metwally H G., 2013. Histological Experimental Study on the Effect of Stem Cell Therapy on Adriamycin Induced Chemobrain. *International Journal of Stem Cells* 6(2):104-112.
 40. Donega V, Nijboer C H, Tilborg G V, Dijkhuizen R M, Kavelaars M, Heijnen C J., 2014. Intranasally administered mesenchymal stem cells promote a regenerative niche for repair

- of neonatal ischemic brain injury. *Experimental Neurology* 261: 53–64.
41. Lim JY, Jeong CH, Jun JA, Kim SM, Ryu CH, Hou Y, Oh W, Chang JW, Jeun SS., 2011. Therapeutic effects of human umbilical cord blood-derived mesenchymal stem cells after intrathecal administration by lumbar puncture in a rat model of cerebral ischemia. *Stem Cell Res Ther.* 2:38.
 42. Ribeiro CA, Fraga JS, Grãos M, Neves NM, Reis RL, Gimble JM, Sousa N, Salgado AJ., 2012. The secretome of stem cells isolated from the adipose tissue and Wharton jelly acts differently on central nervous system derived cell populations. *Stem Cell Res Ther* 2012;3:18.
 43. Da Silva Meirelles L, Fontes AM, Covas DT, Caplan AI., 2009. Mechanisms involved in the therapeutic properties of mesenchymal stem cells. *Cytokine Growth Factor Rev.* 20:419–427.
 44. Ponte A L, Marais E, Gallay N, Langonne A, Delorme B, Herault O, *et al.*, 2007. The in vitro migration capacity of human bone marrow mesenchymal stem cells: comparison of chemokine and growth factor chemotactic activities. *Stem Cells* 25:1737–1745.
 45. Rüster B, Göttig S, Ludwig RJ, Bistrrian R, Müller S, Seifried E, *et al.*, 2006. Mesenchymal stem cells display coordinated rolling and adhesion behavior on endothelial cells. *Blood* 108:3938–3944.
 46. Gaillard PJ, Visser CC, Appeldoorn CC, Rip J., 2012. Enhanced brain drug delivery: safely crossing the blood–brain barrier. *Drug Discov Today Technol.* 9: e155–160.
 47. Schmidt A, Ladage D, Steingen C, Brixius K, Schinköthe T, Klinz FJ, *et al.*, 2006. Mesenchymal stem cells transmigrate over the endothelial barrier. *Eur J Cell Biol* 85:1179–1188.
 48. Steingen C, Brenig F, Baumgartner L, Schmidt J, Schmidt A, Bloch W., 2008. Characterization of key mechanisms in transmigration and invasion mesenchymal stem cells. *J Mol Cell Cardiol.* 44:1072–1084.
 49. Matsushita T, Kibayashi T, Katayama T, Yamashita Y, Suzuki S, Kawamata J, *et al.*, 2011. Mesenchymal stem cells transmigrate across brain microvascular endothelial cell monolayers through transiently formed inter-endo-thelial gaps. *Neurosci Lett.* 502:41–45.
 50. Sharma A, Sane H, Kulkarni P, Yadav J, Gokulchandran N, Biju H, Badhe P., 2015. Cell therapy attempted as a novel approach for chronic traumatic brain injury – a pilot study. *Springer Plus* 4:26.
 51. Siniscalco D, Bradstreet J, Sych N, Antonucci N. 2014. Mesenchymal stem cells in treating autism: Novel insights. *World J Stem Cells* 6(2): 173–178.
 52. Ivanova-Todorova E, Bochev I, Dimitrov R, Belemezova K, Mourdjeva M, Kyurkchiev S, Kinov P, Altankova I, Kyurkchiev D., 2012. Conditioned medium from adipose tissue-derived mesenchymal stem cells induces CD4+FOXP3+ cells and increases IL-10 secretion. *J Biomed Biotechnol*; DOI: 10.1155/2012/295167.
 53. Meirelles S, Fontes M, Covas T, Caplan I., 2009. Mechanisms involved in the therapeutic properties of mesenchymal stem cells. *Cytokine Growth Factor Rev.* 20:419–427.
 54. Prockop D. J., Gregory C. A., Spees J. L., 2003. One strategy for cell and gene therapy: harnessing the power of adult stem cells to repair tissues *Proc. Natl. Acad. Sci. U.S.A.*, 100:11917–11923.
 55. Berardis S, Sattwika P D, Najimi M, Sokal E M., 2015. Use of mesenchymal stem cells to treat liver fibrosis: Current situation and future prospects. *World J Gastroenterol.* 21(3): 742–758.
 56. Jin G, Qiu G, Wu D, Hu Y, Qiao P, Fan C, Gao F., 2013. Allogeneic bone marrow-derived mesenchymal stem cells attenuate hepatic ischemia-reperfusion injury by suppressing oxidative stress and inhibiting apoptosis in rats. *Int. J. Mol. Med.* (6):1395–1401. doi: 10.3892/ijmm.2013.1340.
 57. Lin S L, Kisseleva T, Brenner D. A., Duffield J S., 2008. Pericytes and Perivascular Fibroblasts Are the Primary Source of Collagen-Producing Cells in Obstructive Fibrosis of the Kidney. *Am. J. Pathol.* 173(6):1617–1627.
 58. Haniffa M. A., Collin M. P., Buckley C. D., Dazzi F., 2009. Mesenchymal Stem Cells: The Fibroblasts' New Clothes? *Haematologica.* 94(2):258–263.